Dynamic Scene Graph Representation for Surgical Video

Felix Holm *†1, Ghazal Ghazaei†2, Tobias Czempiel1, Ege Özsoy1, Stefan Saur3, and Nassir Navab1

1Chair for Computer Aided Medical Procedures, Technical University Munich, Germany
2Carl Zeiss AG, Oberkochen, Germany
3Carl Zeiss Meditec AG, Jena, Germany

Abstract

Surgical videos captured from microscopic or endoscopic imaging devices are rich but complex sources of information, depicting different tools and anatomical structures utilized during an extended amount of time. Despite containing crucial workflow information and being commonly recorded in many procedures, usage of surgical videos for automated surgical workflow understanding is still limited. In this work, we exploit scene graphs as a more holistic, semantically meaningful and human-readable way to represent surgical videos while encoding all anatomical structures, tools, and their interactions. To properly evaluate the impact of our solutions, we create a scene graph dataset from semantic segmentations from the CaDIS and CATARACTS datasets. We demonstrate that scene graphs can be leveraged through the use of graph convolutional networks (GCNs) to tackle surgical downstream tasks such as surgical workflow recognition with competitive performance. Moreover, we demonstrate the benefits of surgical scene graphs regarding the explainability and robustness of model decisions, which are crucial in the clinical setting.

1. Introduction

Videos for Surgical Workflow Understanding capture the most integral parts of surgeries from global surgery information to the most atomic actions and tasks. Automated surgical workflow understanding solutions rely on such rich, dense, and complex sources of information to extract useful surgical knowledge such as surgical phases, steps, events as well as instruments and anatomical structures. Surgical Workflow analysis could further promote assisting the surgeons via automated report generation, intraoperative warnings, robotic assistance, workflow optimization, and education.

Accordingly, the field of surgical data science has seen a significant amount of research in the recognition of the surgical workflow, enabled by the introduction of publicly available datasets, such as Cholec80 for laparoscopic cholecystectomy surgeries [16] or CATARACTS for microscopic cataracts surgery [2]. Methods applied in this field range from Convolutional Neural Networks (CNN) [16] to extract latent representations of visual image features to various temporal modeling methods such as Long Short-Term Memory (LSTM) [8], Temporal Convolutions [5], or transformer-based methods [6, 7]. These methods were very successful in steadily improving on the task of surgical workflow recognition, their real-world application in the clinical setting is however still strongly limited. Further advancement in the field of surgical data science is striving for a more holistic and robust understanding of surgery such that tools and anatomies are explicitly recognized and their interactions over time can be meticulously analyzed.

Scene Graphs [13, 17] have been proposed to represent scenes with multiple actors, objects, and relationships between them in a graphical way. Relationships between entities are visualized as edges in a graph where each entity corresponds to a node. Spatio-temporal scene graphs [11] have been used specifically to analyze and differentiate relationships between objects over time. The scene graph representation is a powerful modeling technique to encode a scene on a fine granular level in a human-understandable way and creates the foundation for different complex downstream tasks such as visual question answering or image captioning. As an abstract, but still human-readable representation of a scene, scene graphs also offer benefits in terms of explainability and reasoning, which is highly desirable, especially in the medical domain. Scene graphs have previously been introduced in the medical domain for a holistic understanding of the OR, where the surgical staff and their interactions are modeled [20]. For the 'internal view' of the surgery, such as from an endoscope or surgical mi-

[*] Corresponding Author: felix.holm@tum.de
[†] These authors contributed equally to this work.

croscope, surgical action triplets for cholecystectomy [15] and scene graphs for robotic nephrectomy [10] have been proposed. These methods model the interactions between surgical tools and single target anatomies as graphs but do however not model the full anatomical structure and the relations between them.

In this work, we aim to investigate the utility of surgical scene graphs as a representation of surgical microscopic video for surgical workflow understanding. We utilize scene graphs to represent the complete scene, including all visible anatomies, tools, and their interactions. To avoid the cost of detailed annotations for these experiments, we make use of the CATARACTS and CaDIS datasets. The CATARACTS dataset contains microscopic cataract surgery videos and their corresponding surgical phase annotations to evaluate surgical workflow understanding methods. The CaDIS dataset is a subset of CATARACTS containing semantic segmentation annotations, which allows us to leverage off-the-shelf state-of-the-art semantic segmentation models [14, 4] to localize surgical scene components and further extract their relations to construct a scene graph. The extracted scene graphs are then exploited within a Graph Convolutional-based framework to perform the task of surgical phase recognition. As surgical phases are best presented considering the temporal inter-relations between the frames, we further reinforce our solution with temporal connections among the neighboring static scene graphs to construct a Dynamic Scene Graph (DSG). We highlight the performance of our method and further investigate the benefits of scene graphs in terms of robustness and explainability of predictions.

The features of our suggested solution are as follows:

1. Leveraging off-the-shelf semantic segmentation solutions and available surgical video datasets for creation of a scene graph dataset

2. Implementation of a GCN-based framework to understand and analyze surgical videos via a minimal yet holistic intermediate representation incorporating both spatial and temporal information within surgeries

3. Exploiting the suggested representation on surgical downstream task of phase segmentation to highlight the benefits namely usability, robustness and explainability.

2. Methods

2.1. Semantic Segmentation

We build upon the state-of-the-art solutions in semantic scene segmentation for the CATARACTS dataset, namely OCRNet [14] and Mask2Former [4], to precisely localize surgical scene components. **OCRNet** creates a soft segmentation map by dividing the contextual pixels into a set of soft object regions each assigned to a class. The representations of pixels in an object region are then aggregated to predict the representation of that object region. Finally, each pixel representation is augmented with the object-contextual-representation (OCR) which is a weighted aggregation of all object region representations. **Mask2Former** enhances the extracted feature maps from a backbone ConvNet using a pixel decoder module which outputs high-resolution features. The features are passed into a transformer decoder, creating a set of binary mask and class predictions conditioned on the pixel decoder's features.

2.2. Graph Construction

Static Graph Given an input RGB frame, the segmentation model generates a global 2D segmentation map as visualized in Figure 1.b, which is composed of a set of segments $S = \{s_1, ..., s_n\}$. To generate the scene graph, each segment is represented as a node N_i of the graph $G = (N, E)$ where $N = \{N_1, ..., N_n\}$ and E represents the edges between two nodes. Each node contains a set of features $X \in R^{N \times d}$. We incorporated a variety of features into the scene graphs to study their individual impact. The baseline node feature set only encodes the segment classification from the segmentation model. Additionally, we encode the spatial position of the segment, the relative size of the segment and, in the case of Mask2Former, the instance embedding of each segment. We provide ablation experiments on the features used for graph construction in section 3.3. The undirected edges of the static graph are defined based on the geometrical relation between each two segments (s_i, s_j). If the two segments are connected in the segmentation mask, their corresponding nodes are also connected.

Dynamic Scene Graph (DSG) To leverage temporal relations to create a more holistic spatio-temporal understanding, we aggregate multiple Static Graphs as defined above and connect each node N_i to the nodes belonging to the same class from adjacent temporal steps. The DSG therefore consists of the nodes N_{t_i} and edges E_{t_i} of the static graph of each timestep and the additional temporal connections $E_{t_i \rightarrow t_{i+1}}$, resulting in $G_{DSG} = (N_{t_0} + N_{t_1} + \ldots, E_{t_0} + E_{t_0 \rightarrow t_1} + E_{t_1} + \ldots)$. This allows the changes of each segment s_i over time to be captured and analyzed along the added temporal connections. We vary the number of static graphs that are aggregated to form the dynamic graph, which we refer to as 'Window'. We also consider 'Dilation', where we use static graphs with larger temporal distances to form the dynamic graph to increase the covered temporal context while limiting the graph size. We investigate the impact of these parameters in section 3.3. For dynamic graphs, we also add an encoding of the relative temporal position of each node to the node features, which

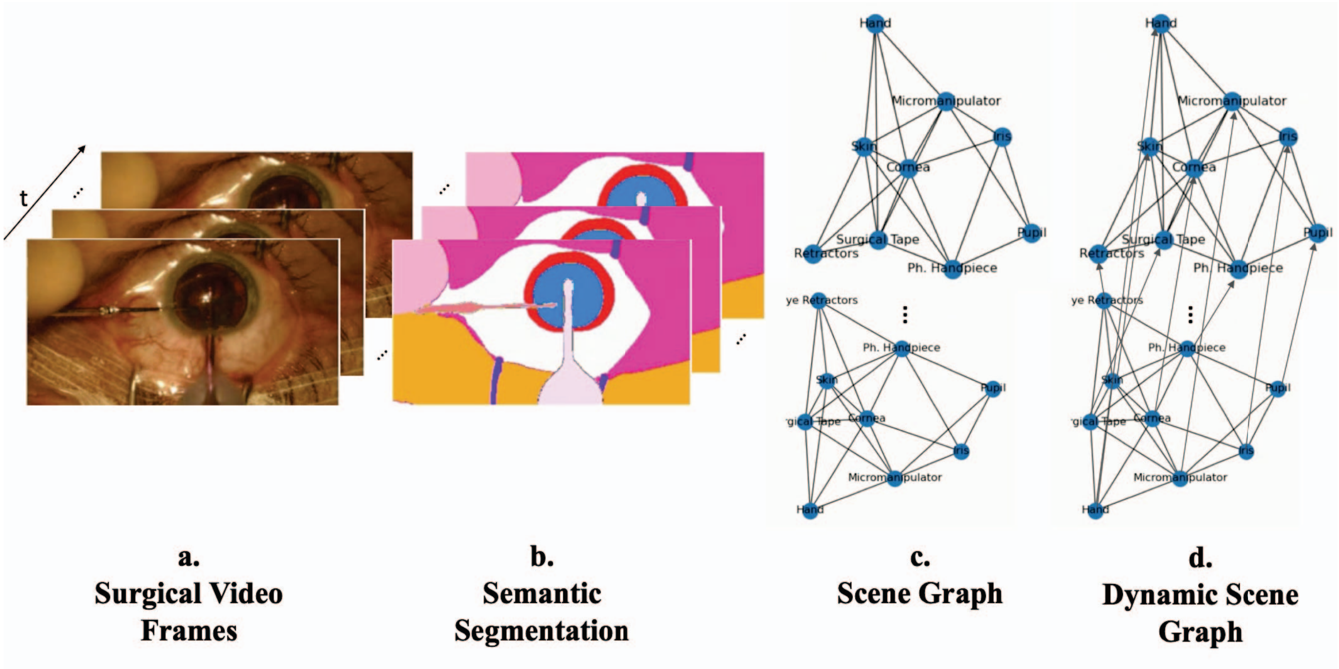

a.
Surgical Video Frames

b.
Semantic Segmentation

c.
Scene Graph

d.
Dynamic Scene Graph

Figure 1. Illustration of surgical Dynamic Scene Graph (DSG) creation: a) Video recorded from the microscopic view of cataract surgery b) semantic segmentation maps indicating anatomical structures and tools c) static scene graphs constructed for each frame highlighting anatomies, tools and their relations d) dynamic scene graph for a sequence of frames indicating the tools, anatomies and their relations across both space (within each frame) and time

we also ablate in section 3.3.

2.3. Graph Convolutional Network

To solve the downstream task of phase recognition, we design a multi-layer graph convolutional network (GCN) [12], taking the scene graph as input. The multi-layer GCN is followed by a global add-pooling layer that aggregates the features from all nodes, followed by a fully connected layer and Softmax$(x_i) = \frac{\exp(x_i)}{\sum_j \exp(x_j)}$ to predict the probabilities for each phase class. We use the cross-entropy loss as our objective function on the labeled frames of videos to optimize the model parameters. Figure 2 shows the overall model structure.

3. Evaluation

3.1. Datasets

CATARACTS [3, 2] consists of 50 cataract surgery videos with a resolution of 1920 × 1080 pixels at 30 frames per second (fps) performed at Brest University Hospital. The average duration of Cataract surgeries within this dataset is 10 minutes and 56 s. The dataset as published for the CATARACTS2020 challenge defines a train set (25 videos), val set (5 videos), and test set (20 videos). Each frame of the videos is annotated with surgical phases by a medical doctor and an ophthalmology nurse. There is a total of 18 phases (excluding the idle phase): 1) Toric Marking, 2) Implant Ejection, 3) Incision, 4) Viscodilatation, 5) Capsulorhexis, 6) Hydrodissetion, 7) Nucleus Breaking, 8) Phacoemulsification, 9) Vitrectomy, 10) Irrigation/Aspiration, 11) Preparing Implant, 12) Manual Aspiration, 13) Implantation, 14) Positioning, 15) OVD Aspiration 16) Suturing, 17) Sealing Control, 18) Wound Hydratation.

CaDIS [9] is a subset of CATARACTS including a total of 4670 pixel-wise annotated images. There are three increasingly granular semantic segmentation tasks defined on CaDIS, from which we take Task II, semantically representing sufficient information for the downstream task of phase segmentation. Task II consists of 17 classes: 0) Pupil 1) Surgical Tape, 2) Hand, 3) Eye Retractors, 4) Iris, 5) Skin, 6) Cornea, 7) Cannula, 8) Capsulorhexis Cystotome, 9) Tissue Forceps, 10) Primary Knife, 11) Phaco Handpiece, 12) Lens Injector, 13) I/A Handpiece, 14) Secondary Knife, 15) Micromanipulator, 16) Capsulorhexis Forceps.

3.2. Implementation details

Segmentation Models We use the provided pre-trained weights for the OCRNet model [14], while we trained the Mask2Former model with the Swin small backbone on the CaDIS dataset using the implementation provided by [1]. The segmentation models are evaluated on the full CATARACTS dataset (at 1 fps) to create semantic segmentation maps, out of which static scene graphs are generated.

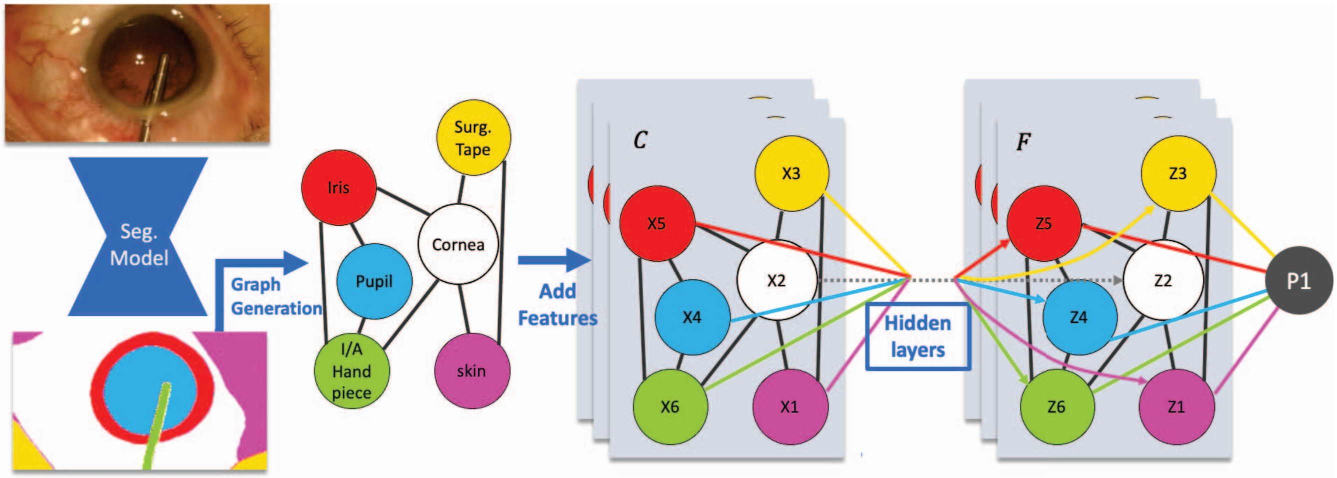

Figure 2. Overview of the proposed pipeline: Video frames are segmented based on their semantic classes s_i which can then be leveraged for construction of a scene graph with each semantic class as a node N_i. Each node will be connected to another if they are adjacent to each other in the segmentation map. The nodes can be further reinforced with custom features. The scene graph is then passed into a multi-layer GCN trained on the downstream task of surgical phase recognition. C and F indicate the number of input and feature maps respectively.

Graph Construction The scene graphs are constructed and populated with features extracted from the segmentation depending on the experiment. The sizes of these feature vectors are: 15 (segment classification), 16 (spatial position), 1 (segment size), 16 (temporal position), 100 (M2F class query embedding).

Graph Convolutional Network Our scene graph-based phase segmentation model consists of 8 graph convolution layers with hidden dimensions of 64, 64, 128, 128, 192, 128, 64, 64, and a fully convolutional layer. Since the model and constructed scene graph dataset are relatively small, the GCN can be trained without GPU hardware acceleration. This highlights another strength of scene graphs as a lightweight video representation.

3.3. Results and Discussion

Semantic Segmentation Table 1 highlights the results of Mask2Former compared with state of the art, OCRNet. Mask2Former performs better mean Intersection over Union (mIoU) overall and more specifically indicates prior performance for localization and segmentation of instruments which is crucial for the downstream task of phase segmentation. It is worth to note that both models still present noisy pixelwise segmentation and misclassification for scene representations that are more distinct from the majority of dataset distribution.

Graph Representation Table 2 illustrates the impact of features on our static scene graph within extensive ablation studies, from only having class embedding to enriching the graph with temporal and positional encoding, segmentation size, and finally class query embedding. Our results suggest that although incorporating additional information is beneficial, the most minimal graph still captures sufficient information from the surgical scene enabling comparable phase recognition. This validates our assumption that surgical scene graphs can provide a minimal yet holistic representation of the scene and effectively be used for downstream tasks.

Table 1. Semantic segmentation results of used models on Task II of CaDIS [9] test set

	OCRNet [14]	Mask2Former [4]
mIoU (Anatomy)	**90.63**	83.14
mIoU (Instruments)	76.89	**83.58**
mIoU (All classes)	79.09	**80.97**

Robustness We constructed our scene graphs based on the output of both OCRNet [14] and Mask2Former [4] semantic segmentation maps (see Table 2). We show that both methods can effectively learn the downstream task, although both backbones provide imperfect segmentation results (see Table 1 and Figure 3), which demonstrates the inherent robustness of the scene graph representation. As Figure 3 indicates, the phase segmentation results remain consistent along the frames a to i although the semantic segmentation results from Mask2Former indicate incosistencies in this scenario. It can be observed that parts of pupil, iris and lense injector are missed in frame 3 b and the wrong instrument category is predicted in frame 3 g. Furthermore, the static scene graph representation indicates a stable scene representation not sensitive to imperfections of semantic segmentation maps which is essential for a reliable surgical workflow analysis.

Table 2. Experiments on static and dynamic scene graph construction for phase segmentation of CATARACTS. Mask2Former abbreviated as M2F. Node Features: Spatial Position, Segmentation Size, M2F Embedding, Temporal Position

	Segmentation	Node Features					
Graph	Backbone	Spatial	Size	Emb	Temp	Accuracy	F_1
Static	M2F					64.34	50.04
Static	M2F	✓				65.36	51.08
Static	M2F		✓			64.92	48.91
Static	M2F			✓		64.47	49.05
Static	M2F	✓	✓			65.56	52.24
Static	M2F	✓		✓		66.00	52.62
Static	M2F		✓	✓		66.04	52.82
Static	M2F	✓	✓	✓		**66.42**	**53.90**
Dynamic	OCRNet	✓	✓			54.02	39.64
Dynamic	OCRNet	✓	✓		✓	71.99	63.51
Dynamic	M2F	✓	✓			60.05	48.85
Dynamic	M2F	✓	✓		✓	73.77	64.93
Dynamic	M2F	✓	✓	✓		58.26	47.41
Dynamic	M2F	✓	✓	✓	✓	**75.15**	**68.56**

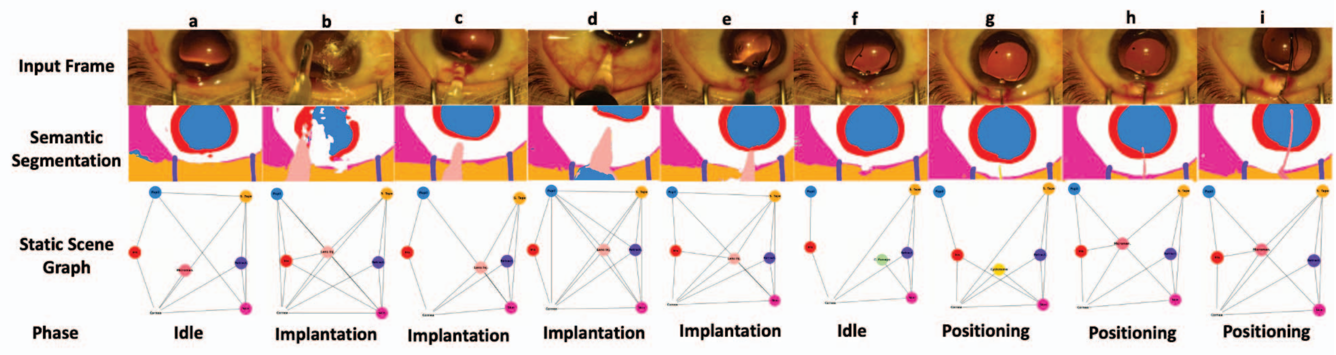

Figure 3. A demonstration of robustness of static scene graphs and more specifically prediction of downstream task of phase segmenatation to noisy semantic segmentation of frames both in localization (b) and classification (g) of objects.

Temporality Table 3 shows the impact of the length of temporal sequences and learned context via temporal dilation. Our results suggest that a temporal context of 90s is optimal for classifying phases within Cataract surgery. Considering the duration of phases generally between 5 s and 2 min respectively, this temporal context seems appropriate.

Performance As there are no published benchmarks available on the CATARACTS phase segmentation dataset as publicly released, we provide a comparison to DeepPhase [19]. DeepPhase is based on the same videos of CATARACTS but uses a different set of labels with 14 phases, from which some are not included in our ground truth and vice-versa. The results we can show here (Table 4) indicate that our scene graph-based model performs competitively.

Table 3. Experiments on size and stride for the temporal window.

Window	Dilation	Context	Accuracy	F_1
30	1	30s	71.72	62.61
30	3	90s	**75.15**	**68.56**
30	5	150s	73.24	65.67
30	10	300s	73.99	65.27
100	1	100s	74.83	68.27
100	3	300s	73.15	64.75
100	5	500s	71.24	62.44
150	1	150s	73.98	66.56
150	3	450s	70.32	63.93
150	5	750s	69.01	60.88

Explainability Finally, we highlight that scene graphs can provide additional insights into the model decisions via direct access to the nodes and the relations between them. Figure 4 highlights the relations and nodes in the DSG that

Table 4. Comparison to DeepPhase [19] on phase recognition on CATARACTS.

Temporality	Model	Input to temporal Model	Accuracy	F_1
LSTM	DeepPhase [19]	Binary	68.75	68.50
LSTM	DeepPhase [19]	Features	78.28	74.92
GRU	DeepPhase [19]	Binary	71.61	67.33
GRU	DeepPhase [19]	Features	68.96	66.62
Dynamic Graph	M2F + GCN	SG + Embeddings	76.86	67.41

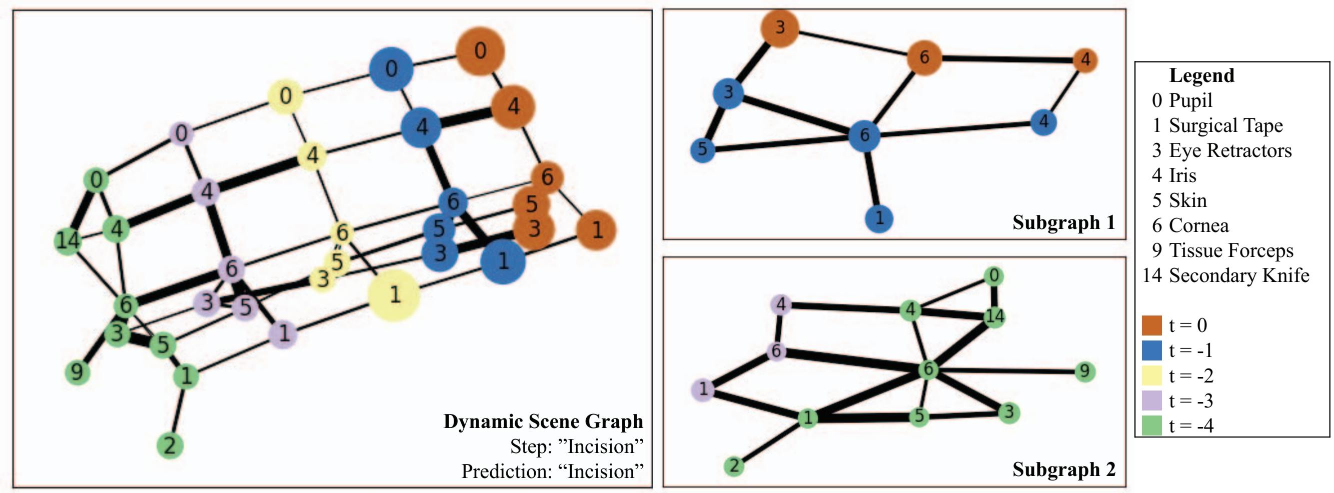

Figure 4. Explanations for Predictions based on the DSG generated with [18]. Edge Thickness corresponding to Edge Importance, Node Size corresponding to Node Importance. The Dynamic Scene Graph shows five timesteps, indicated by color. Two important subgraphs can be identified, which are shown on the right.

were most important for the prediction. Because of the nature of the scene graphs, these explanations are directly semantically meaningful. E.g., the interaction between the Secondary Knife (14) and Pupil (0), and Tissue Forceps (9) and and Cornea (6) are important for the prediction, even when they occured 5 timesteps in the past. Other realtions that represent temporal connections are highlighted as important as well, such as the relation between the Iris (4) in timestep 0 and -1. This indicates that the changes over time between these timesteps were important for the prediction. From the edge and node importance, two subgraphs can be identified that are shown in Figure 4 on the right. Subgraph 1 consists mostly of anatomy such as Iris, Pupil and Cornea and their changes over the last timestep. Subgraph 2 shows the tool interaction with Secondary Knife and Tissue Forceps and its relation with the surrounding anatomy. This shows our model considers both these spatially and temporally defined regions of the DSG as important for the final correct prediction of step "Incision". We consider the ability for explanation of predictions a major benefit of DSG over latent vector representations, which is crucial in the medical setting to gain the trust of clinicians and patients and ensure their safety through quality control.

4. Conclusion

We demonstrate a new method to leverage surgical scene graphs for surgical workflow recognition in cataract surgery. To achieve this, we generate a new scene graph dataset from semantic segmentations based on the CaDIS dataset. We develop a dynamic GCN-based framework to leverage scene graphs for surgical workflow understanding by learning a minimal yet holistic intermediate representation of surgical videos. Our approach proves to be robust, as we apply it to various imperfect segmentation backbones. Furthermore, we provide visualizations of the model's reasoning, highlighting the most important elements of the scene graph, which shows the human understandability and explainability of our approach. We thereby demonstrate the benefits of scene graphs as a representation of surgical video in future surgical data science applications.

References

[1] Mask2former. https://huggingface.co/docs/transformers/model_doc/mask2former, 2022. Accessed: 2023-02-24. 3

[2] Hassan Al Hajj, Mathieu Lamard, Pierre-Henri Conze, Soumali Roychowdhury, Xiaowei Hu, Gabija Maršalkaitė, Odysseas Zisimopoulos, Muneer Ahmad Dedmari, Fenqiang Zhao, Jonas Prellberg, et al. Cataracts: Challenge on automatic tool annotation for cataract surgery. *Medical image analysis*, 52:24–41, 2019. 1, 3

[3] Hassan ALHAJJ, Mathieu Lamard, Pierre-henri Conze, Béatrice Cochener, and Gwenolé Quellec. Cataracts, 2021. 3

[4] Bowen Cheng, Ishan Misra, Alexander G Schwing, Alexander Kirillov, and Rohit Girdhar. Masked-attention mask transformer for universal image segmentation. In *Proceedings of the IEEE/CVF Conference on Computer Vision and Pattern Recognition*, pages 1290–1299, 2022. 2, 4

[5] Tobias Czempiel, Magdalini Paschali, Matthias Keicher, Walter Simson, Hubertus Feussner, Seong Tae Kim, and Nassir Navab. TeCNO: Surgical Phase Recognition with Multi-stage Temporal Convolutional Networks. In Anne L. Martel, Purang Abolmaesumi, Danail Stoyanov, Diana Mateus, Maria A. Zuluaga, S. Kevin Zhou, Daniel Racoceanu, and Leo Joskowicz, editors, *Medical Image Computing and Computer Assisted Intervention – MICCAI 2020*, volume 12263, pages 343–352. Springer International Publishing, Cham, 2020. Series Title: Lecture Notes in Computer Science. 1

[6] Tobias Czempiel, Magdalini Paschali, Daniel Ostler, Seong Tae Kim, Benjamin Busam, and Nassir Navab. OperA: Attention-Regularized Transformers for Surgical Phase Recognition. *arXiv:2103.03873 [cs]*, Mar. 2021. arXiv: 2103.03873. 1

[7] Xiaojie Gao, Yueming Jin, Yong-Hao Long, Qi Dou, and Pheng-Ann Heng. Trans-svnet: Accurate phase recognition from surgical videos via hybrid embedding aggregation transformer. *CoRR*, abs/2103.09712, 2021. 1

[8] Carly Garrow, Karl-Friedrich Kowalewski, Linhong Li, Martin Wagner, Mona Schmidt, Sandy Engelhardt, Daniel Hashimoto, Hannes Kenngott, Sebastian Bodenstedt, Stefanie Speidel, Beat Müller, and Felix Nickel. Machine learning for surgical phase recognition a systematic review. *Annals of Surgery*, Publish Ahead of Print, 11 2020. 1

[9] Maria Grammatikopoulou, Evangello Flouty, Abdolrahim Kadkhodamohammadi, Gwenol'e Quellec, Andre Chow, Jean Nehme, Imanol Luengo, and Danail Stoyanov. Cadis: Cataract dataset for image segmentation. *arXiv preprint arXiv:1906.11586*, 2019. 3, 4

[10] Mobarakol Islam, Lalithkumar Seenivasan, Lim Chwee Ming, and Hongliang Ren. Learning and Reasoning with the Graph Structure Representation in Robotic Surgery. In Anne L. Martel, Purang Abolmaesumi, Danail Stoyanov, Diana Mateus, Maria A. Zuluaga, S. Kevin Zhou, Daniel Racoceanu, and Leo Joskowicz, editors, *Medical Image Computing and Computer Assisted Intervention – MICCAI 2020*, Lecture Notes in Computer Science, pages 627–636, Cham, 2020. Springer International Publishing. 2

[11] Jingwei Ji, Ranjay Krishna, Li Fei-Fei, and Juan Carlos Niebles. Action genome: Actions as composition of spatio-temporal scene graphs. *CoRR*, abs/1912.06992, 2019. 1

[12] Thomas N Kipf and Max Welling. Semi-supervised classification with graph convolutional networks. *arXiv preprint arXiv:1609.02907*, 2016. 3

[13] Ranjay Krishna, Yuke Zhu, Oliver Groth, Justin Johnson, Kenji Hata, Joshua Kravitz, Stephanie Chen, Yannis Kalantidis, Li-Jia Li, David A. Shamma, Michael S. Bernstein, and Li Fei-Fei. Visual genome: Connecting language and vision using crowdsourced dense image annotations. *CoRR*, abs/1602.07332, 2016. 1

[14] Theodoros Pissas, Claudio S Ravasio, Lyndon Da Cruz, and Christos Bergeles. Effective semantic segmentation in cataract surgery: What matters most? In *Medical Image Computing and Computer Assisted Intervention–MICCAI 2021: 24th International Conference, Strasbourg, France, September 27–October 1, 2021, Proceedings, Part IV 24*, pages 509–518. Springer, 2021. 2, 3, 4

[15] Saurav Sharma, Chinedu Innocent Nwoye, Didier Mutter, and Nicolas Padoy. Rendezvous in Time: An Attention-based Temporal Fusion approach for Surgical Triplet Recognition, Nov. 2022. arXiv:2211.16963 [cs]. 2

[16] Andru P. Twinanda, Sherif Shehata, Didier Mutter, Jacques Marescaux, Michel de Mathelin, and Nicolas Padoy. EndoNet: A Deep Architecture for Recognition Tasks on Laparoscopic Videos. *arXiv:1602.03012 [cs]*, May 2016. arXiv: 1602.03012. 1

[17] Danfei Xu, Yuke Zhu, Christopher B. Choy, and Li Fei-Fei. Scene graph generation by iterative message passing. *CoRR*, abs/1701.02426, 2017. 1

[18] Zhitao Ying, Dylan Bourgeois, Jiaxuan You, Marinka Zitnik, and Jure Leskovec. Gnnexplainer: Generating explanations for graph neural networks. *Advances in neural information processing systems*, 32, 2019. 6

[19] Odysseas Zisimopoulos, Evangello Flouty, Imanol Luengo, Petros Giataganas, Jean Nehme, Andre Chow, and Danail Stoyanov. Deepphase: surgical phase recognition in cataracts videos. In *Medical Image Computing and Computer Assisted Intervention–MICCAI 2018: 21st International Conference, Granada, Spain, September 16-20, 2018, Proceedings, Part IV 11*, pages 265–272. Springer, 2018. 5, 6

[20] Ege Özsoy, Evin Pınar Örnek, Ulrich Eck, Tobias Czempiel, Federico Tombari, and Nassir Navab. 4d-or: Semantic scene graphs for or domain modeling. In *International Conference on Medical Image Computing and Computer-Assisted Intervention*. Springer, 2022. 1